ELSEVIER

Thermochimica Acta 256 (1995) 271–280

thermochimica acta

Thermal decomposition kinetics of some new unsaturated polyesters

M.M.M. Abd El-Wahab

Chemistry Department, Faculty of Science, Assiut University, Assiut, Egypt

Received 17 January 1994; accepted 22 August 1994

Abstract

Studies of non-isothermal decomposition of some new diarylidene-isopropylpipridinone polyesters were carried out using TGA measurements in air atmosphere. TG and DTG investigations revealed that the decomposition of these polymers proceeds in four stages. Analysis of TG curves proves the advantages of this technique in quickly providing valid information about the thermal decomposition kinetics of the polymers. The kinetic parameters such as activation energy E_a, pre-exponential factor A, entropy of activation S^*, free energy of activation G and enthalpy of activation H for all polymers at different decomposition stages are determined. The data show that the thermal stabilities of these polymers are in the order **I** > **II** > **IV** > **III**. In addition, the effect of the presence of a substituent $-OCH_3$ group upon the thermal properties of polymers is discussed.

Keywords: Decomposition; DTG; Non-isothermal; Polyester; Polymer; TGA

1. Introduction

Throughout the literature, there are many papers concerning the synthesis and characterization of various new high performance polymers [1–6]. However, only a small amount of work has been published on the thermal behaviour and kinetic analysis of the polymers [7–10]. The determination of the kinetic parameters of the polymers provides important additional information for their use and applications as new materials.

Non-isothermal methods have been used extensively for the determination of kinetic parameters. Many authors have employed different computational methods among which the Freeman–Carroll [11], Coats–Redfern [12], Horowitz–Metzger

SSDI 0040-6031(94)02183-X

[13], Doyle [14] modified by Zsako [15] and Šatava–Škvarà [16] methods are well known and have been tested by several researchers [17–19].

In the present work, we study the thermogravimetry and kinetic analysis of non-isothermal decomposition for new diarylidene-isopropylpipridinone polyesters.

2. Experimental

2.1. Materials

The polymers under investigation were prepared as described recently [6]. In a three-necked flask equipped with a mechanical stirrer, dry nitrogen inlet and outlet, and dropper, a mixture of 3.5 mmol dibenzylidene isopropylpiperidinone, 30 ml methylene chloride and sodium hydroxide solution (8 mmol) was introduced. After mixing, 3.5 mmol of acid chlorides dissolved in 30 ml methylene chloride was added over a period of 2 min at 25°C and vigorously stirred. After complete addition of acid chloride, stirring was continued for 1–2 h, and a highly yellowish solid polymer separated out. The solid polymer was filtered off, washed with water, then with hot alcohol, and then dried under reduced pressure (1 mmHg) at 80°C for 2 days.

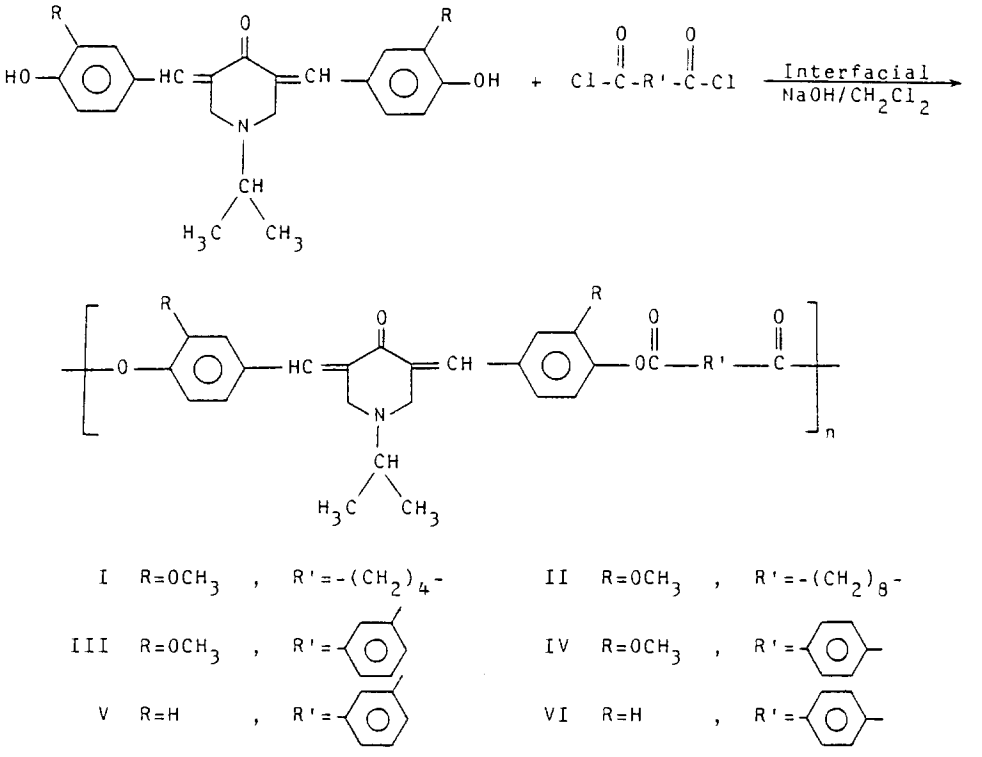

I R=OCH3 , R'=-(CH2)4- II R=OCH3 , R'=-(CH2)8-

III R=OCH3 , R'= IV R=OCH3 , R'=

V R=H , R'= VI R=H , R'=

Scheme 1.

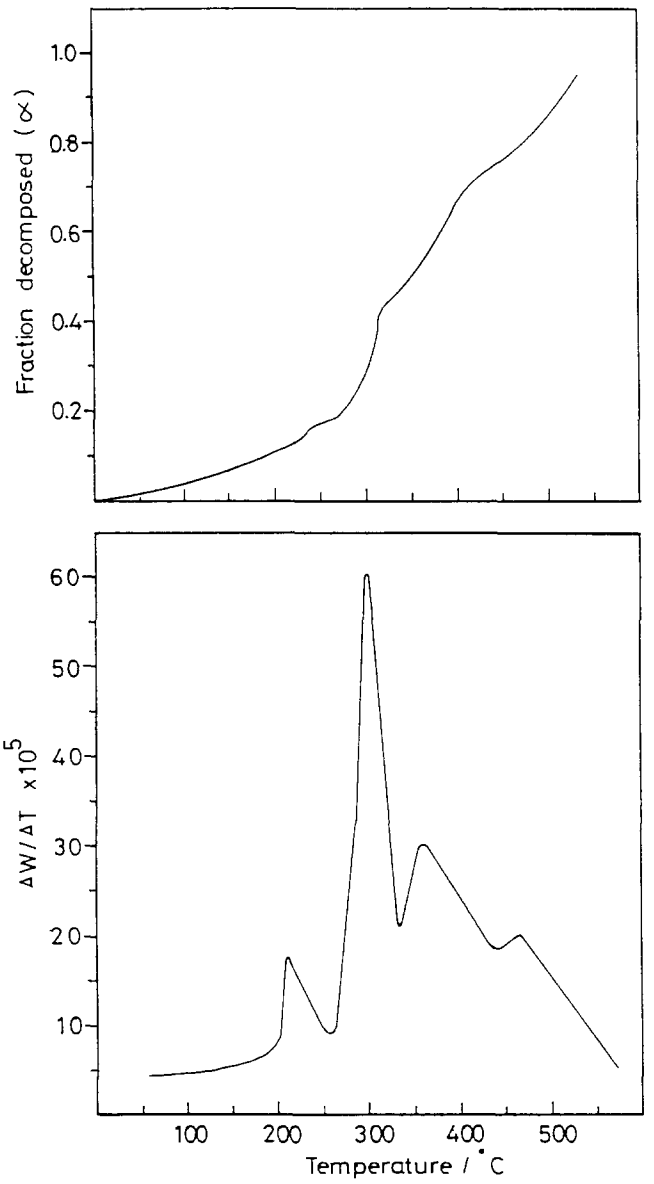

Fig. 1. TG and DTG curves for the thermal decomposition of polymer **I**.

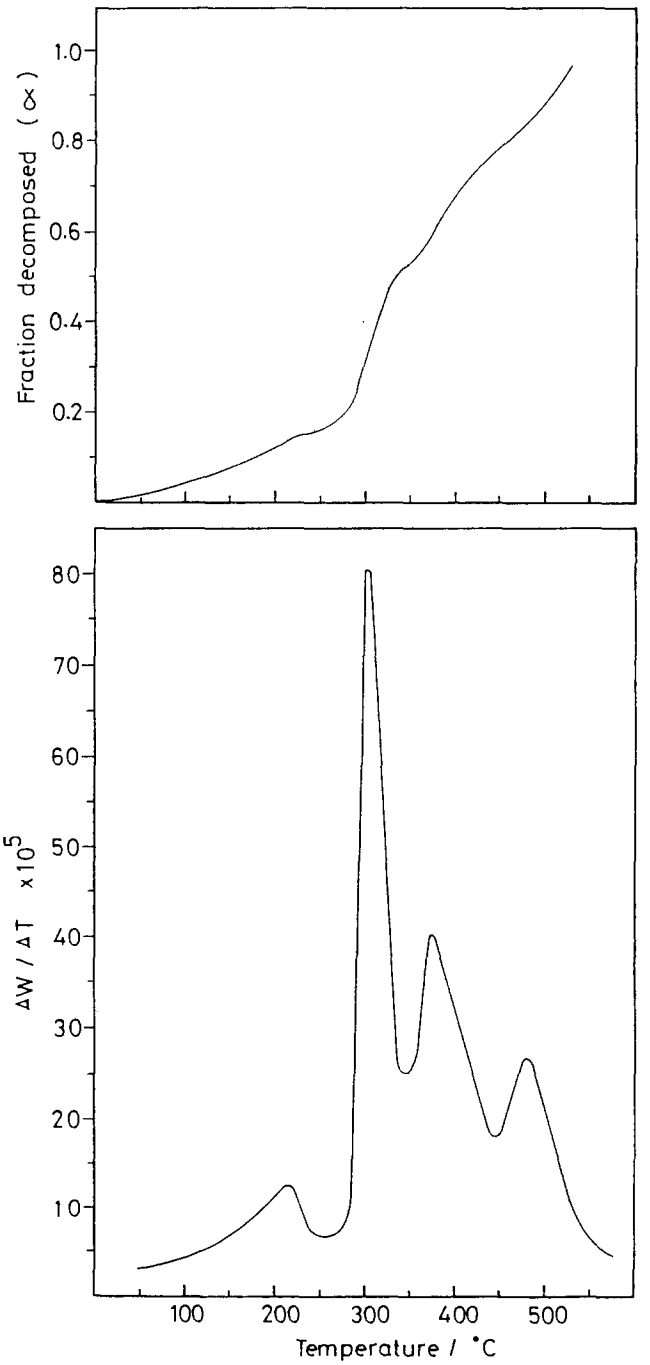

Fig. 2. TG and DTG curves for the thermal decomposition of polymer **IV**.

2.2. Techniques

Thermogravimetric analysis (TG) was performed with a Sartorius electric thermobalance. Samples (100 mg) were placed in the platinum basket suspended from the arm of the balance by means of a Pyrex wire. The mass change was recorded up to 550°C, with a heating rate of 10°C min^{-1} under air atmosphere.

3. Results and discussion

Thermogravimetric analyses for all samples were obtained in the temperature range $25°C < t < 550°C$. All the samples show the same thermal decomposition behaviour. Figs. 1 and 2 show the TG and DTG curves for samples **I** and **IV**. The curves are characterized by four mass-loss stages. These stages correspond to the following processes [20]: (i) cleavage of –OCO– bonds and evolution of CO_2, which is detected by GC, (ii) oxidative degradation of substituted groups R and R′, (iii) rupture of N–C bonds and degradation of piperidinone ring, and (iv) decomposition of the aromatic residues with simultaneous scission of different kinds of covalent linkage to form a char as end product. Table 1 shows the percentage mass loss corresponding to each decomposition stage of the polymers. The temperatures corresponding to various α values are given in Table 2.

From these tables, some conclusions can be drawn.

Table 1
Percentage mass loss accompanying the four decomposition stages of the polymers

Polymer	Stage	Mass loss/%	
		Found	Calc.
I	(i)	14.6	15.0
	(ii)	23.6	24.0
	(iii)	27.8	28.5
	(iv)	17.6	18.0
II	(i)	13.2	13.4
	(ii)	31.9	32.4
	(iii)	25.0	25.5
	(iv)	15.2	15.7
III and **IV**	(i)	14.4	14.3
	(ii)	28.0	27.6
	(iii)	27.1	27.4
	(iv)	16.7	16.8
V and **VI**	(i)	15.8	16.3
	(ii)	16.9	17.2
	(iii)	30.6	31.1
	(iv)	18.0	18.8

Table 2
Temperatures in °C corresponding to various α values of the polymers

α	I	II	III	IV	V	VI
0.15	234	232	208	230	215	235
0.30	301	299	295	297	303	322
0.45	328	326	322	324	348	370
0.60	381	377	372	374	414	417
0.75	440	436	430	433	468	470
0.90	513	508	501	504	519	522

(i) Polymer **I** is more thermally stable than polymer **II**. This stability can be attributed to the more rigid structure in polymer **I** compared with the long chain, more thermally labile, polymer **II**.

(ii) The aliphatic based polymers (**I**, **II**) are more stable than the aromatic based polymers (**III**, **IV**). This could be ascribed to the high stability of aryl radical formed by decarbonation upon cleavage of –OCO– bonds.

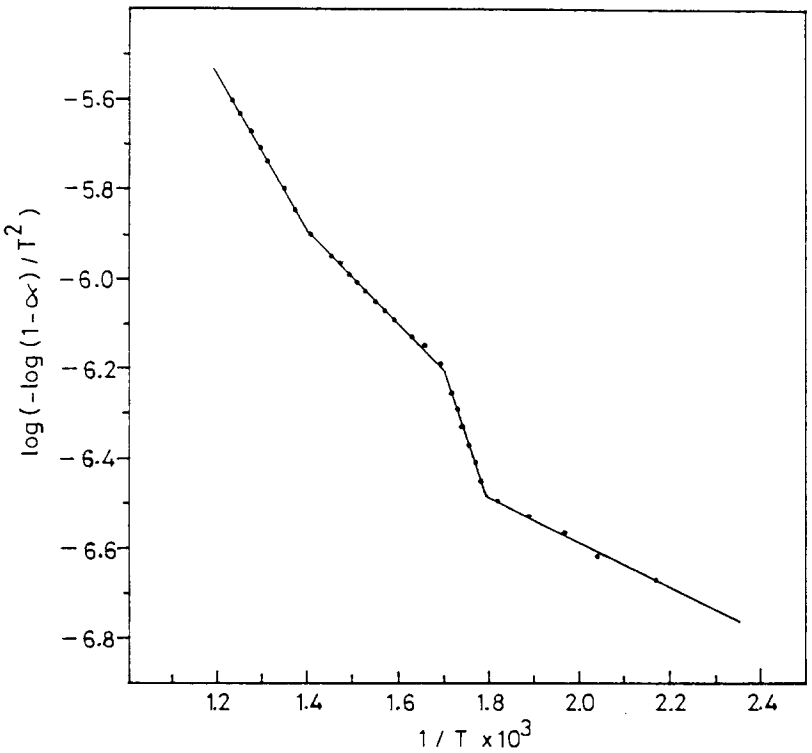

Fig. 3. Coats–Redfern plot for the non-isothermal decomposition of polymer **I**.

(iii) Polymer **IV** is more thermally stable than polymer **III** due to the steric hindrance in the meta-disubstituted polymer **III** compared with the para-disubstituted polymer **IV**.

(iv) Polymers **V** and **VI** are more stable than polymers **III** and **IV** respectively. The lower relative stability can be attributed to the presence of an $-OCH_3$ donor group which decreases the stability of –OCO– towards oxidation.

To evaluate the kinetic data from the TG curve, different mathematical kinetic methods [11–16] were used. Our goal in this type of non-isothermal analysis is to estimate the reaction order. This can easily be achieved by observing the best straight line fitting the data with the exact solution for each method. For our analysis of the data on the thermal decomposition of the sample, it was found that the appropriate equation which fits the data is in general a typical integral which firstly can be formulated as

$$\int_0^{\alpha} d\alpha(1-\alpha)^n = A/\phi \int_0^{T} \exp(-E_a/RT)\, dt \qquad (1)$$

where α is the reaction fraction decomposed, ϕ is the heating rate, T is the absolute temperature at time t, n is the order of reaction, R is the gas constant in J mol^{-1} K^{-1} and E_a is the activation energy in J mol^{-1}.

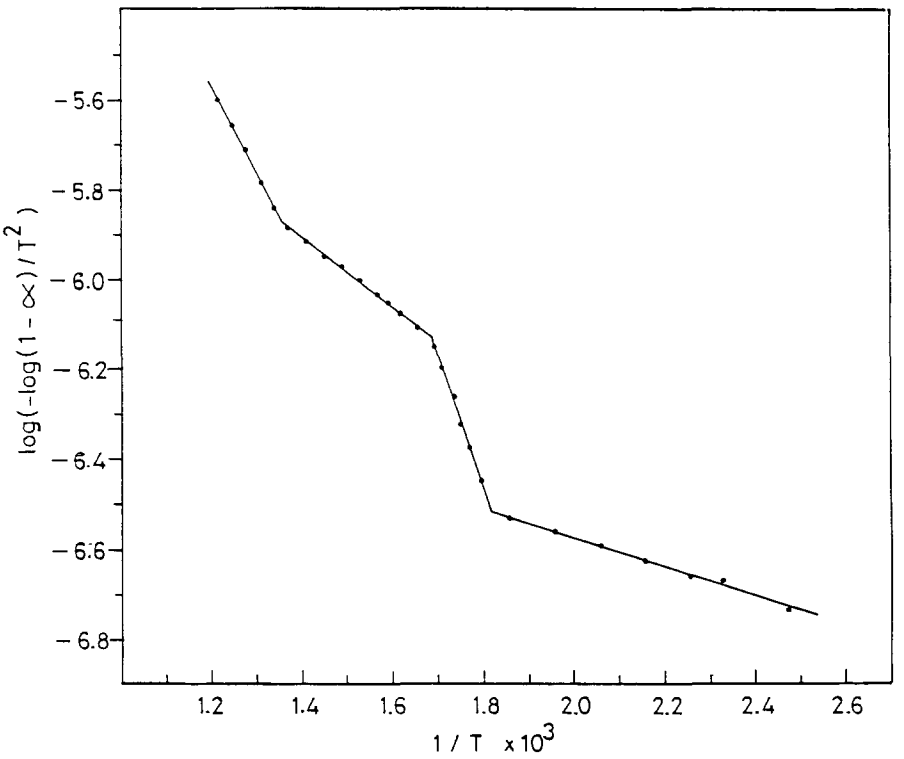

Fig. 4. Coats–Redfern plot for the non-isothermal decomposition of polymer **IV**.

Generally, the term $d\alpha(1-\alpha)^n$ has two different solutions: $1-(1-\alpha)^{1-n}/1-n$ for $n \neq 1$, and $-\log(1-\alpha)$ for $n=1$.

The right hand side in Eq. (1) has the solution

$$\frac{ART^2}{\phi E_a}\left(\frac{1-2RT}{E_a}\right)\exp(-E_a/RT)$$

and after taking logarithms we obtain for $n \neq 1$

$$\log\left(\frac{1-(1-\alpha)^{1-n}}{T^2(1-n)}\right)=\log\left(\frac{AR}{\phi E_a}\frac{(1-2RT)}{E_a}\right)-\frac{E_a}{2.303RT}$$

Table 3
Kinetic parameters for the non-isothermal decomposition of the polymers

Range/°C	E/(kJ mol^{-1})	A/(s^{-1})	S^*/(J mol^{-1} K^{-1})	G/(kJ mol^{-1})	H/(kJ mol^{-1})
I					
200–255	9.6	4.9×10^{-4}	−0.530	9.86	5.58
260–320	68.0	0.6×10^{2}	−0.332	68.19	63.24
325–440	19.9	1.4×10^{-2}	−0.318	20.11	14.55
440–550	33.8	2.3×10^{-1}	−0.431	34.12	27.66
II					
190–255	10.1	6.4×10^{-4}	−0.472	10.33	6.00
260–345	37.4	9.4×10^{-1}	−0.360	37.61	32.68
350–450	15.8	5.3×10^{-3}	−0.442	16.09	10.41
500–530	59.4	0.2×10^{2}	−0.318	59.65	52.77
III					
180–210	21.7	2.9×10^{-2}	−0.440	21.91	17.77
270–335	34.7	4.9×10^{-1}	−0.388	34.92	29.98
340–480	16.7	6.7×10^{-3}	−0.471	17.01	11.19
480–540	38.0	4.8×10^{-1}	−0.402	38.31	31.66
IV					
125–240	6.0	1.4×10^{-4}	−0.529	6.25	2.03
265–330	57.8	1.3×10^{2}	−0.304	57.98	52.99
340–450	15.1	4.6×10^{-3}	−0.476	15.41	9.71
455–527	36.1	3.4×10^{-1}	−0.408	36.41	29.84
V					
175–285	10.1	7.5×10^{-4}	−0.571	10.39	5.92
290–360	21.7	1.8×10^{-2}	−0.514	22.01	16.69
365–490	12.6	1.8×10^{-3}	−0.561	13.00	6.67
495–550	79.3	6.3×10^{3}	−0.278	79.52	72.79
VI					
180–275	4.5	6.2×10^{-5}	−0.618	4.81	0.32
285–345	21.8	1.5×10^{-2}	−0.517	22.10	17.04
355–500	26.3	3.8×10^{-2}	−0.502	26.64	20.75
510–540	95.3	5.8×10^{3}	−0.288	95.53	88.67

and for $n = 1$ we obtain

$$\log\left(\frac{-\log(1-\alpha)}{T^2}\right) = \log\left(\frac{AR}{\phi E_a}\frac{(1-2RT)}{E_a}\right) - \frac{E_a}{2.303RT}$$

In ordinary thermal decomposition reactions the term $\log(AR/\phi E_a)(1-(2RT/E_a))$ is practically constant, and plots of $\log[(1-(1-\alpha)^{1-n})/(T^2(1-n))]$ versus $1/T$ for $n \neq 1$ and $\log[-\log(1-\alpha)/T^2]$ versus $1/T$ for $n = 1$ result in a straight line with a slope of $E_a/2.303R$ and intercept of $\log(AR/\phi E_a)$ where the value $1-2RT/E_a \approx 1$.

Plots of $\log[-\log(1-\alpha)/T^2]$ against $1/T$ for samples **I** and **IV** have been drawn in Figs. 3 and 4, whereby a good linear correlation associated with breaking of the straight lines was obtained. Such breaking indicates a four-stage decomposition process as discussed before. The E_a values for each stage were calculated from the corresponding slope, and A was obtained from the intercept.

The entropy of activation S^*, the free energy of activation G, and the enthalpy of activation H were calculated starting from [21]

$$S^* = 2.303R \log Ah/kT_i$$

where h and k are the Planck and Boltzmann constants, respectively, and T_i is the peak temperature from the DTG curve. As the reaction rate depends mainly on the free energy of activation, the entropy of activation S^* should decide the magnitude of G according to $G = E - T_i S^*$. The enthalpy of activation was calculated using $E \approx H + RT_i$. Hence $H \approx E - RT_i$.

The kinetic parameters for the non-isothermal decomposition and the temperature range in which each decomposition step occurs are summarized in Table 3.

References

[1] J.A. Mikroyannidis, Eur. Polym. J., 25 (1989) 557.
[2] J.A. Mikroyannidis, J. Polym. Sci., 29 (1991) 411.
[3] J.A. Mikroyannidis, J. Polym. Sci., 29 (1991) 881.
[4] M.A. Abd-Alla and R.M. Mahfouz, J. Appl. Polym. Sci., 42 (1991) 2225.
[5] M.A. Abd-Alla, M.F. El-Zohry, K.I. Aly and M.M.M. Abd El-Wahab, J. Appl. Polym. Sci., 47 (1993) 323.
[6] K.I. Aly and A.A. Geies, High Perf. Polym., 4 (1992) 187.
[7] B.L. Stump and W.J. Snyder, High Perf. Polym., 1 (1989) 247.
[8] L.H. Tagle and F.R. Diaz, J. Macromol. Sci.-Chem. A, 28 (1991) 397.
[9] M.M.M. Abd El-Wahab and M.A. Abd-Alla, High Perf. Polym., 4 (1992) 215.
[10] M.A. Abd-Alla and M.M.M. Abd El-Wahab, Thermochim. Acta, 222 (1993) 255.
[11] E.S. Freeman and B. Carroll, J. Chem., 62 (1958) 394.
[12] A.W. Coats and J.P. Redfern, Nature, 201 (1964) 68.
[13] H.H. Horowitz and G. Metzger, Anal. Chem., 35 (1963) 1464.
[14] C.D. Doyle, J. Appl. Polym. Sci., 15 (1961) 285.
[15] J. Zsakò, J. Phys. Chem., 72 (1968) 2406.
[16] V. Šatava and F. Škvarà, J. Am. Ceram. Soc., 52 (1969) 591.
[17] D.T.Y. Chen. J. Therm. Anal., 6 (1974) 109.
[18] D.T.Y. Chen and P.H. Fong, J. Therm. Anal., 8 (1975) 295.

[19] P.H. Fong and D.T.Y. Chen., J. Therm. Anal., 8 (1975) 305.
[20] R.C. Weast (Ed.), C.R.C. Handbook of Chemistry and Physics, 62nd edn., C.R.C. Press, FL 1981–1982, p. F-193.
[21] S. Glasstone, A Textbook of Physical Chemistry, 2nd edn., Macmillan, Bombay, India, 1974.